



A THEORETICAL ANALYSIS OF MULTI-MODAL BASS-TRAPPING RESONATORS COUPLED TO CONTROL-ROOM ACOUSTICS

PACS: 43.55.Cs

Antunes, José¹; Inácio, Octávio²

¹Instituto Tecnológico Nuclear, Applied Dynamics Laboratory, Estrada Nacional 10, 2686 Sacavém, Portugal; jantunes@itn.pt

²ESMAE-Instituto Politécnico do Porto, Musical Acoustics Laboratory, R. da Alegria 503, 4000-045 Porto, Portugal; Octaviolnacio@esmae-ipp.pt

ABSTRACT

Helmholtz resonators are often applied for the sound equalisation of control rooms in recording studios, through adequate levelling of the low frequency acoustic modal room responses. The number of controlled acoustic modes depends on the central frequency and damping of resonators, as well as on the modal density of the controlled system within the resonators frequency range. In a recent paper we proposed to improve the efficiency of such devices by, instead of using basic Helmholtz resonators develop shape optimized multi-modal resonators in order to cope with a larger number of intrusive room modes. In spite of the promising results thus obtained, further work is needed to demonstrate the feasibility of such approach. The present paper is a further step in that direction by analysing the acoustics of the fully coupled room/resonators system. More specifically, using a substructure computational approach we theoretically derive the coupled acoustical modes of control rooms fitted with several optimized multi-mode resonators.

INTRODUCTION

During the last decades, there has been some controversy on which should be the best design principles for sound control rooms, concerning namely their reverberation and sound diffusion characteristics. Nevertheless, there is a general agreement that strong room resonance responses should be avoided, particularly at the lower frequencies. Indeed, the unbalance between over-enhancement of sound at these modal frequencies and the absence of room response at anti-resonances originates a detrimental lack of uniformity of the room acoustic response and undue sound colouration. This effect is more pronounced for the frequency range where modal density and modal damping are low. Additionally, the room dimensions may be such that packs of modes occur in certain frequency ranges, not only maximizing the resonance effect but also creating separation between different peaks in the room frequency response.

These problems have often been tackled, with more or less efficiency, by the use of Helmholtz resonators, membrane panels or tube-traps, among others. The uncoupled resonance behaviour of these bass control devices is typically focused on a central frequency of maximum sound absorption which spreads over a determined bandwidth. The number of controlled acoustic modes depends on several factors among which are the central resonance frequency chosen, the modal density in the controlled frequency range, damping, and the ratio of the resonator to room volumes. The degree of attenuation of the resonance effect is dependent not only on the number of such devices used, but also on their location in the room, ideally close to pressure antinodes of the mode to control. Helmholtz resonators have been particularly used in many different applications where an accurate control of a single frequency is desired. These resonators have been thoroughly studied since the 19th century beginning with the work of Helmholtz. More recently, several researchers became interested in the design and physical behaviour of such systems [1,2], on the effect of basic geometry changing on the resonant frequency [3,4], and on the acoustical coupling between the resonator and the room [5,6], to mention a few.

In a recent paper [7] we suggested that the efficiency of such resonators may be significantly improved if, instead of using basic Helmholtz or devices with uniform cross-section, more complex shape-optimized resonators are used in order to cope with a larger number of undesirable acoustic modes. Hence we applied optimization techniques in order to obtain optimal shapes for such devices so that they resonate at a target set of acoustic eigenvalues, within imposed physical and/or geometrical constraints. However, a complete

analysis of this problem has to consider the frequency shifts and room modeshape distortion arising from the acoustical coupling between the room and the resonator, as well as the viscous boundary layer absorption effects which account for the damping at the entrance of the resonators. Therefore, in spite of the promising preliminary results obtained, further work is needed to demonstrate the feasibility of such approach.

In the present paper we analyse the acoustics of the fully coupled room/resonator(s) system. A theoretical method for computing the complex (dissipative) coupled acoustical modes of a control room fitted with one or several multi-mode resonators is developed and then illustrated with an example. Such problem may be tackled using brute-force numerical techniques, for instance the FE or BE methods, coupled with a suitable model for the acoustical damping phenomena. However such approach is highly computer intensive, involving thousands of degrees of freedom, and hence is ill adapted to the extensive modal computations called by an optimization procedure. Hence we develop here a substructure computational method, the coupled acoustical modes being computed from the reduced modal basis sets of the isolated room and resonator(s), assumed closed at their interface(s). Such approach is highly advantageous: (a) It leads to manipulation of a few hundred modes at most; (b) When optimizing the shape and location of the resonator(s) the modal basis of the basic room only has to be computed once. In contrast with the approach developed in the excellent paper by Fahy and Schofield [5], the method proposed here applies to multi-mode resonators, as intended, in the spirit of [7]. It can be viewed an extension of the penalty formulation presented by Axisa & Antunes [8], suitable for coupled volumes with significant interface damping.

CONSERVATIVE MODEL FOR COUPLED ROOM / RESONATORS

We will first address the basic conservative acoustical problem, which will then be extended to include dissipative phenomena.

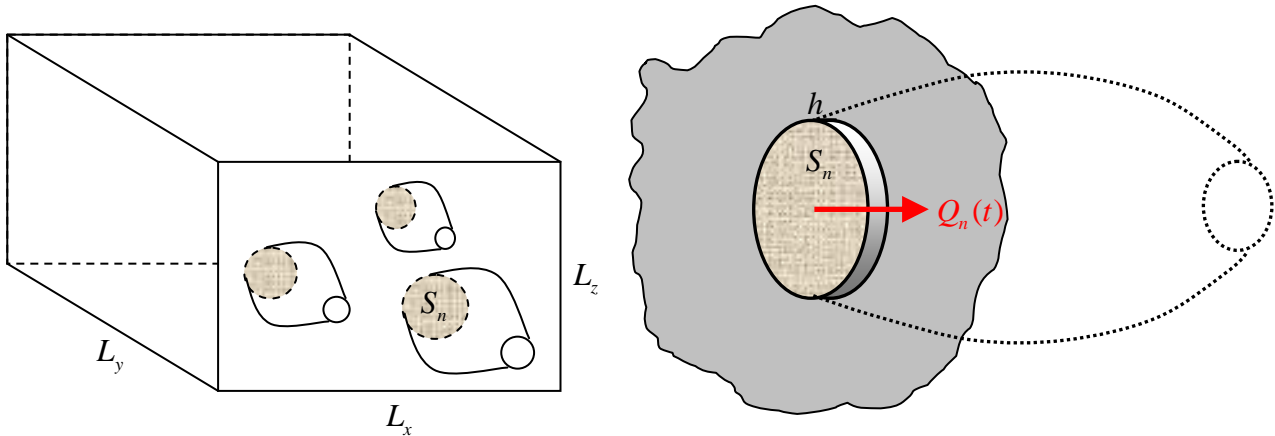


Figure 1.- (a) Basic sound control room coupled with multi-mode resonators; (b) Interface model

Theoretical formulation

Figure 1 shows the sketch of a control room of generic shape, coupled with N resonating multi-mode devices. One may write an inhomogeneous wave equation for the room – see for instance [1,5,8]:

$$\frac{1}{c_0^2} \frac{\partial^2}{\partial t^2} p_r(\vec{s}_r, t) - \nabla^2 p_r(\vec{s}_r, t) = \rho_0 \left[\frac{\partial Q_e(t)}{\partial t} \delta(\vec{s}_r - \vec{s}_r^e) + \sum_{n=1}^N \frac{\partial Q_n(t)}{\partial t} \delta(\vec{s}_r - \vec{s}_r^n) \right] \quad (1)$$

Here the excitation $Q_e(t)$ is a given volume-velocity point-source. The $Q_n(t) = S_n \dot{\xi}_n(t)$ are localized sources related to the acoustical flow between the resonator(s) and the room, where $\xi_n(t)$ are the (cross-section averaged) acoustical displacements in the associated interfaces S_n at locations \vec{s}_r^n . Therefore (1) is written:

$$\ddot{p}_r(\vec{s}_r, t) - c_0^2 \nabla^2 p_r(\vec{s}_r, t) = c_0^2 \rho_0 \left[\dot{Q}_e(t) \delta(\vec{s}_r - \vec{s}_r^e) + \sum_{n=1}^N S_n \ddot{\xi}_n(t) \delta(\vec{s}_r - \vec{s}_r^n) \right] \quad (2)$$

And for each coupled resonator we have:

$$\ddot{p}_n(\vec{s}_n, t) - c_0^2 \nabla^2 p_n(\vec{s}_n, t) = -c_0^2 \rho_0 S_n \ddot{\xi}_n(t) \delta(\vec{s}_n - \vec{s}_n^i) \quad ; \quad n = 1, 2, \dots, N \quad (3)$$

Equations (2-3) must be supplemented with suitable closure conditions, to insure the compatibility of the acoustical flows at the resonator interfaces. We will assume that these are of finite depth h , with both S_n and h much smaller than the acoustic wavelengths of interest, so that the flow may be postulated incompressible in the small interface volumes $v_n = S_n h$. Hence the dynamical balance of the fluid inside them:

$$\rho_0 S_n h \ddot{\xi}_n(t) = S_n [p_n(\bar{s}_n^r, t) - p_r(\bar{s}_r^n, t)] \Rightarrow \ddot{\xi}_n(t) = \frac{1}{\rho_0 h} [p_n(\bar{s}_n^r, t) - p_r(\bar{s}_r^n, t)] ; n = 1, 2, \dots, N \quad (4)$$

This closed set of equations may be further simplified by feeding (4) into (2-3). We then obtain the equivalent compact form:

$$\ddot{p}_r(\bar{s}_r, t) - c_0^2 \nabla^2 p_r(\bar{s}_r, t) = \frac{c_0^2}{h} \sum_{n=1}^N S_n [p_n(\bar{s}_n, t) \delta(\bar{s}_n - \bar{s}_r^r) - p_r(\bar{s}_r, t) \delta(\bar{s}_r - \bar{s}_r^n)] \quad (5)$$

$$\ddot{p}_n(\bar{s}_n, t) - c_0^2 \nabla^2 p_n(\bar{s}_n, t) = -\frac{c_0^2}{h} S_n [p_n(\bar{s}_n, t) \delta(\bar{s}_n - \bar{s}_r^r) - p_r(\bar{s}_r, t) \delta(\bar{s}_r - \bar{s}_r^n)] ; n = 1, 2, \dots, N \quad (6)$$

In a view completely different from (2-4), equations (5-6) may be seen as a penalty formulation for the coupled problem, by taking $K_n \equiv c_0^2 S_n / h$ as penalty parameters which enforce the pressure fields of the two connected subsystems to be near-identical at each interface. Actually, notice that for small depth h the values of K_n will be quite large, as they should, so that both the volume-source formulation (2-4) and the equivalent system (5-6) are consistent with the penalty approach developed in [8]. We will use (2-4) in the following, because this formulation is more amenable to address the general dissipative problem.

Modal formulation

Equations (2-4) will be now discretized using modal projection. As usual, the pressure fields are defined as:

$$p_r(\bar{s}_r, t) = \sum_{m=1}^{M_r} \phi_m^{(r)}(\bar{s}_r) P_m^{(r)}(t) \quad \text{and} \quad p_n(\bar{s}_n, t) = \sum_{m=1}^{M_n} \phi_m^{(n)}(\bar{s}_n) P_m^{(n)}(t) ; n = 1, 2, \dots, N \quad (7)$$

where $\phi_m^{(r)}$ and $\phi_m^{(n)}$ are the pressure modeshapes respectively of the isolated (closed) room and N (closed) resonators. Replacing (7) into (2) and projecting the resulting equation on the room modes we obtain:

$$\begin{aligned} & \iiint_{V_r} \left(\sum_{m=1}^{M_r} \phi_m^{(r)}(\bar{s}_r) \ddot{P}_m^{(r)}(t) \right) \phi_k^{(r)}(\bar{s}_r) dv - c_0^2 \iiint_{V_r} \left(\sum_{m=1}^{M_r} [\nabla^2 \phi_m^{(r)}(\bar{s}_r)] P_m^{(r)}(t) \right) \phi_k^{(r)}(\bar{s}_r) dv = \\ & = c_0^2 \rho_0 \left[\dot{Q}_e(t) \iiint_{V_r} \phi_k^{(r)}(\bar{s}_r) \delta(\bar{s}_r - \bar{s}_r^e) dv + \sum_{n=1}^N S_n \ddot{\xi}_n(t) \iiint_{V_r} \phi_k^{(r)}(\bar{s}_r) \delta(\bar{s}_r - \bar{s}_r^n) dv \right] ; k = 1, 2, \dots, M_r \end{aligned} \quad (8)$$

and, accounting for the modal orthogonality, all cross-terms in the right-hand side of (8) vanish, except for the terms $m=k$, so that:

$$A_k^{(r)} \ddot{P}_k^{(r)}(t) + B_k^{(r)} P_k^{(r)}(t) = c_0^2 \rho_0 \left[\dot{Q}_e(t) \phi_k^{(r)}(\bar{s}_r^e) + \sum_{n=1}^N S_n \ddot{\xi}_n(t) \phi_k^{(r)}(\bar{s}_r^n) \right] ; k = 1, 2, \dots, M_r \quad (9)$$

with:

$$A_k^{(r)} = \iiint_{V_r} [\phi_k^{(r)}(\bar{s}_r)]^2 dv ; B_k^{(r)} = -c_0^2 \iiint_{V_r} [\nabla^2 \phi_k^{(r)}(\bar{s}_r)] \phi_k^{(r)}(\bar{s}_r) dv = (\omega_k^{(r)})^2 A_k^{(r)} ; k = 1, 2, \dots, M_r \quad (10)$$

Similarly, from (3), we obtain for each resonator:

$$A_k^{(n)} \ddot{P}_k^{(n)}(t) + B_k^{(n)} P_k^{(n)}(t) = -c_0^2 \rho_0 S_n \ddot{\xi}_n(t) \phi_k^{(n)}(\bar{s}_r^n) ; k = 1, 2, \dots, M_n ; n = 1, 2, \dots, N \quad (11)$$

with:

$$A_k^{(n)} = \iiint_{V_n} [\phi_k^{(n)}(\bar{s}_n)]^2 dv ; B_k^{(n)} = -c_0^2 \iiint_{V_n} [\nabla^2 \phi_k^{(n)}(\bar{s}_n)] \phi_k^{(n)}(\bar{s}_n) dv = (\omega_k^{(n)})^2 A_k^{(n)} ; k = 1, 2, \dots, M_n ; n = 1, 2, \dots, N \quad (12)$$

Finally, replacing (7) into the compatibility equations (4):

$$\ddot{\xi}_n(t) = \frac{1}{\rho_0 h} \left[\left(\sum_{m=1}^{M_n} \phi_m^{(n)}(\bar{s}_r^n) P_m^{(n)}(t) \right) - \left(\sum_{m=1}^{M_r} \phi_m^{(r)}(\bar{s}_r^r) P_m^{(r)}(t) \right) \right] ; n = 1, 2, \dots, N \quad (13)$$

We now assemble equations (9-13) into convenient matrix form, consisting on $M_r + \sum_{n=1}^N M_n + N$ equations:

$$\begin{bmatrix} A^0 & \dots & 0 \\ \vdots & \ddots & \vdots \\ 0 & \dots & A_k^0 \\ & & A^1 & \dots & 0 \\ & & \vdots & \ddots & \vdots \\ & & 0 & \dots & A_k^1 \\ & & & & \ddots & \ddots \\ & & & & & A^N & \dots & 0 \\ & & & & & \vdots & \ddots & \vdots \\ & & & & & 0 & \dots & A_k^N \end{bmatrix} \begin{bmatrix} \ddot{P}_1^0(t) \\ \vdots \\ \ddot{P}_k^0(t) \\ \ddot{P}_1^1(t) \\ \vdots \\ \ddot{P}_k^1(t) \\ \vdots \\ \ddot{P}_1^N(t) \\ \vdots \\ \ddot{P}_k^N(t) \\ \ddot{\xi}_1(t) \\ \vdots \\ \ddot{\xi}_N(t) \end{bmatrix} + \begin{bmatrix} -C_{d1}^0(\bar{s}) & \dots & -C_{dM}^0(\bar{s}) \\ \vdots & \ddots & \vdots \\ -C_{d1}^1(\bar{s}) & \dots & -C_{dM}^1(\bar{s}) \\ C_{d1}^1(\bar{s}) & \dots & 0 \\ \vdots & \ddots & \vdots \\ C_{d1}^N(\bar{s}) & \dots & 0 \\ \vdots & \ddots & \vdots \\ 0 & \dots & C_{dM}^N(\bar{s}) \\ \vdots & \ddots & \vdots \\ 1 & \dots & 0 \\ \vdots & \ddots & \vdots \\ 0 & \dots & 1 \end{bmatrix} \begin{bmatrix} P_1^0(t) \\ \vdots \\ P_k^0(t) \\ P_1^1(t) \\ \vdots \\ P_k^1(t) \\ \vdots \\ P_1^N(t) \\ \vdots \\ P_k^N(t) \\ \xi_1(t) \\ \vdots \\ \xi_N(t) \end{bmatrix} + \begin{bmatrix} B^0 & \dots & 0 \\ \vdots & \ddots & \vdots \\ 0 & \dots & B_k^0 \\ & & B^1 & \dots & 0 \\ & & \vdots & \ddots & \vdots \\ & & 0 & \dots & B_k^1 \\ & & & & \ddots & \ddots \\ & & & & & B^N & \dots & 0 \\ & & & & & \vdots & \ddots & \vdots \\ & & & & & 0 & \dots & B_k^N \\ & & & & & & & \ddots & \ddots \\ D_{d1}^0(\bar{s}) & \dots & D_{dM}^0(\bar{s}) & -D_{d1}^0(\bar{s}) & \dots & -D_{dM}^0(\bar{s}) & \dots & 0 & \dots & 0 & 0 & \dots & 0 \\ \vdots & \ddots & \vdots & \vdots & \ddots & \vdots & \dots & \vdots & \ddots & \vdots & \vdots & \ddots & \vdots \\ D_{d1}^N(\bar{s}) & \dots & D_{dM}^N(\bar{s}) & 0 & \dots & 0 & \dots & -D_{d1}^N(\bar{s}) & \dots & -D_{dM}^N(\bar{s}) & 0 & \dots & 0 \end{bmatrix} \begin{bmatrix} P_1^0(t) \\ \vdots \\ P_k^0(t) \\ P_1^1(t) \\ \vdots \\ P_k^1(t) \\ \vdots \\ P_1^N(t) \\ \vdots \\ P_k^N(t) \\ \xi_1(t) \\ \vdots \\ \xi_N(t) \end{bmatrix} = \begin{bmatrix} \dot{Q}_e(t) \\ \vdots \\ \dot{Q}_e(t) \\ \vdots \\ \dot{Q}_e(t) \\ \vdots \\ \dot{Q}_e(t) \\ \vdots \\ \dot{Q}_e(t) \\ \vdots \\ \dot{Q}_e(t) \\ \vdots \\ \dot{Q}_e(t) \end{bmatrix} \quad (14)$$

Here only the relevant non-zero sub-matrices are highlighted and we have introduced parameters $C_n = c_0^2 \rho_0 S_n$ and $D_0 = (\rho_0 h)^{-1}$. The coupled system matrix equation (14) may be written in compact form as:

$$\begin{bmatrix} [A^{(r)}] & [0] & \dots & [0] & [C^{(r)}] \\ [0] & [A^{(n)}] & \dots & [0] & [C^{(n)}] \\ \vdots & \vdots & \ddots & \vdots & \vdots \\ [0] & [0] & \dots & [A^{(m)}] & [C^{(m)}] \\ [0] & [0] & \dots & [0] & [1] \end{bmatrix} \begin{Bmatrix} \{\ddot{P}^{(r)}(t)\} \\ \{\ddot{P}^{(n)}(t)\} \\ \vdots \\ \{\ddot{P}^{(m)}(t)\} \\ \{\xi(t)\} \end{Bmatrix} + \begin{bmatrix} [B^{(r)}] & [0] & \dots & [0] & [0] \\ [0] & [B^{(n)}] & \dots & [0] & [0] \\ \vdots & \vdots & \ddots & \vdots & \vdots \\ [0] & [0] & \dots & [B^{(m)}] & [0] \\ [D^{(r)}] & [D^{(n)}] & \dots & [D^{(m)}] & [0] \end{bmatrix} \begin{Bmatrix} \{P^{(r)}(t)\} \\ \{P^{(n)}(t)\} \\ \vdots \\ \{P^{(m)}(t)\} \\ \{\xi(t)\} \end{Bmatrix} = \begin{Bmatrix} \{\phi^{(r)}(\bar{s}_r)\} \\ \{0\} \\ \vdots \\ \{0\} \\ \{0\} \end{Bmatrix} c_0^2 \rho_0 \dot{Q}_e(t) \quad (15)$$

or:

$$[A]\{\ddot{V}(t)\} + [B]\{V(t)\} = \{E\} c_0^2 \rho_0 \dot{Q}_e(t) \quad (16)$$

Then, assuming eigen-solutions of the form $\{V(t)\} = \{V_s\} \exp(\lambda_s t)$, the homogeneous equation stemming from (16) leads to the classic eigenvalue problem:

$$([B] + \lambda_s^2 [A])\{V_s\} = \{0\} \quad (17)$$

where $\lambda_s \equiv \omega_s$ are the circular frequencies of the coupled modes and $\{V_s\}$ are the corresponding eigenvectors. Finally the coupled modeshapes $\psi_s^{(c)}$ are computed by modal recombination (within the complete domain \bar{s}_c) of the original sub-system modeshapes:

$$\psi_s^{(c)}(\bar{s}_c) = \{\Phi^{(r)}(\bar{s}_r)\}^T \{V_s^{(r)}\} \cup \sum_{n=1}^N \{\Phi^{(n)}(\bar{s}_n)\}^T \{V_s^{(n)}\} \quad (18)$$

where $\{V_s^{(r)}\}$ are the eigenvector components pertaining to the set of room modeshapes $\{\Phi^{(r)}(\bar{s}_r)\}$, while the $\{V_s^{(n)}\}$ are those pertaining to the N sets of resonator modeshapes $\{\Phi^{(n)}(\bar{s}_n)\}$.

Illustrative example

As a representative but simple illustration of the preceding formulation, the following will be addressed, consisting on a “shoe-box” room with dimensions $L_x = 5$, $L_y = 9$ and $L_z = 4$ m, which is coupled with 2 additional resonators. These are simple cylinders with length $L = 3$ m and diameter $D = 0.5$ m, located respectively at points $\bar{s}_1^r = [1.25 \ 0.0 \ 2.8]$ and $\bar{s}_2^r = [3.75 \ 0.0 \ 2.8]$. The interface areas, each with $S = 0.20 \text{ m}^2$, are those of the cylinders cross-section. The values of physical parameters are $c_0 = 343 \text{ m/s}$ and $\rho_0 = 1.25 \text{ Kg/m}^3$.

The modes of both these sub-systems can be written analytically. For the closed room, modal frequencies and modeshapes are given as:

$$f_{ijk}^{(r)} = \frac{c_0}{2} \left[\left(\frac{i}{L_x} \right)^2 + \left(\frac{j}{L_y} \right)^2 + \left(\frac{k}{L_z} \right)^2 \right]^{1/2} ; \quad \phi_{ijk}^{(r)}(x, y, z) = \cos \frac{i\pi x}{L_x} \cos \frac{j\pi y}{L_y} \cos \frac{k\pi z}{L_z} \quad (i, j, k = 0, 1, 2, \dots) \quad (19)$$

both being sorted in order of increasing frequency and the truncated beyond a given frequency, typically 1.5~2 times the maximum frequency of interest for the coupled modes to be computed. The cylinders are modelled in terms of plane waves, so that for the closed resonators:

$$f_m^{(r)} = \frac{c_0 m}{2L} ; \quad \phi_m^{(n)}(s) = \cos \frac{m\pi s}{L} \quad (m = 0, 1, 2, \dots) \quad (20)$$

Computation of the modal coefficients (10) and (12) is straightforward, leading to:

$$A_{ijk}^{(r)} = L_x L_y L_z / 2^{P_r(i, j, k)} ; \quad B_{ijk}^{(r)} = (\omega_{ijk}^{(r)})^2 A_{ijk}^{(r)} ; \quad A_m^{(n)} = SL / 2^{P_n(m)} ; \quad B_m^{(n)} = (\omega_m^{(n)})^2 A_m^{(n)} \quad (21)$$

where $P_r(i, j, k)$ and $P_n(m)$ are the number of non-zero indexes for each mode (19) and (20). Computation of the coupling coefficients in sub-matrices $[C^{(r)}]$, $[C^{(n)}]$, $[D^{(r)}]$ and $[D^{(n)}]$ of (15) presents no difficulty.

Table 1.- Modal frequencies of the isolated closed sub-systems

Mode	1	2	3	4	5	6	7	8	9	10	11	12	13
Room	0.0	19.06	34.30	38.11	39.24	42.88	46.92	51.27	54.91	57.17	57.36	58.12	66.67
Resonators	0.0	57.17	114.3										

Table 1 displays the first modal frequencies of the independent sub-systems, closed at their interfaces. A more extensive view of these modal bases is shown in Figure 2(a). Computation of the system coupled modes was performed using all modes in the range 0~200 Hz, namely 208 room modes and 4 resonator modes, leading to matrix sizes of 218x218 in Equation (15). The coupled system modal frequencies are

shown in Table 2 and Figure 2(b), computed using the present model and the FEM, respectively. The finite-element model, which is taken as a comparing reference, called for more than 10^5 degrees of freedom, partly due to the refined mesh needed in the room/resonator interface transition regions – see Figure 3. In this particular case the present approach was faster by three orders of magnitude.

Table 2.- Modal frequencies of the coupled system

Mode	1	2	3	4	5	6	7	8	9	10
Present approach	0.0	18.87	29.26	29.72	34.50	38.34	39.44	42.92	46.97	51.31
FEM	0.0	18.83	26.62	27.07	34.43	38.28	39.39	42.92	46.97	51.31

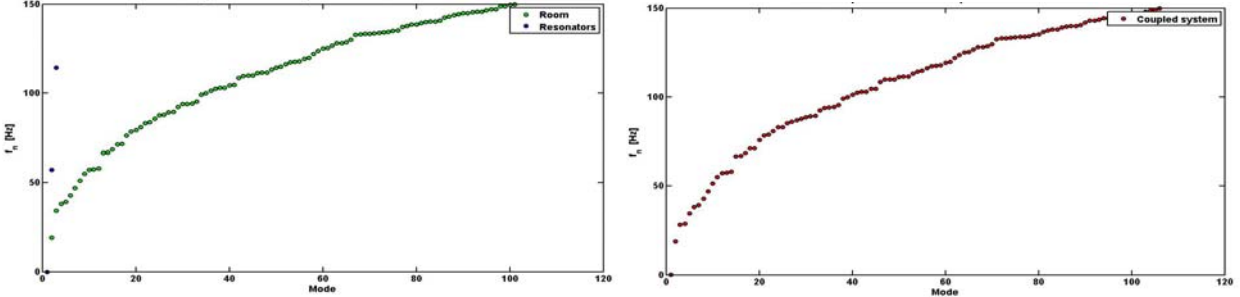


Figure 2.- (a) Modal frequencies of the isolated (closed) room and resonators; (b) Modal frequencies of the coupled system

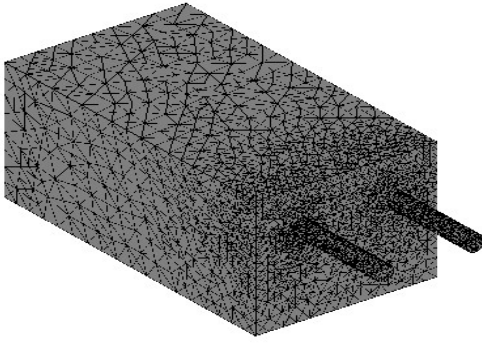


Figure 3.- Mesh used in the FEM computations

The results in Table 2 show negligible differences for all the computed coupled modes, except for modes 3 and 4 (where all acoustical “activity” lays on the resonators), which display a near-node of pressure at the interfaces – see Figure 4.

Because such dynamical behaviour is at the opposite of the boundary conditions in the starting modal basis of this formulation, these particular modes are more sensitive to the modal truncation in the computational model. Indeed, increasing further the frequency range of computation resulted in decreasing these errors. Furthermore, the results obtained are almost insensitive to the (small) value of the interface depth, also as expected, which was in the present computations taken as $h = 0.001$.

Figure 4 displays the first nine (non-zero frequency) coupled modeshapes computed by the present method, which are nearly indistinguishable from those stemming from the FEM computations. These plots clearly highlight the modes where room/resonators coupling is significant and those where these subsystems remain decoupled.

DISSIPATIVE MODEL FOR COUPLED ROOM / RESONATORS

Lack of space prevent us from presenting here in detail the dissipative case, of particular relevance for applications, however the main ideas will be sketched. Dissipative phenomena will be modelled: (a) Through modal damping coefficients in equations (9) and (11), to cover the energy absorption in rooms and acoustic volumes through the usual dissipative processes (air viscosity, wall and furniture absorption, etc.). Such damping coefficients $\zeta_k^{(r)}$ and $\zeta_k^{(n)}$ are typically low, a few percent at most, and may somewhat abusively be postulated as the result of “proportional” damping. In other words, the modal basis of the decoupled subsystems are postulated to be real, as far as these phenomena are concerned. Hence:

$$A_k^{(r)} \ddot{P}_k^{(r)}(t) + Z_k^{(r)} \dot{P}_k^{(r)}(t) + B_k^{(r)} P_k^{(r)}(t) = c_0^2 \rho_0 \left[\dot{Q}_e(t) \phi_k^{(r)}(\bar{S}_r^e) + \sum_{n=1}^N S_n \ddot{\xi}_n(t) \phi_k^{(r)}(\bar{S}_r^n) \right] ; \quad k = 1, 2, \dots, M_r \quad (22)$$

$$A_k^{(n)} \ddot{P}_k^{(n)}(t) + Z_k^{(n)} \dot{P}_k^{(n)}(t) + B_k^{(n)} P_k^{(n)}(t) = -c_0^2 \rho_0 S_n \ddot{\xi}_n(t) \phi_k^{(n)}(\bar{S}_r^n) ; \quad k = 1, 2, \dots, M_n ; \quad n = 1, 2, \dots, N \quad (23)$$

(b) At the room/resonator interfaces, strong dissipation may arise due to local viscous phenomena, which may be significantly increased by the use of damping porous materials with specific “acoustic resistance” (per unit area) η_n - see Figure 1. Then, at each interface, the dynamic balance equation (4) is replaced by:

$$\ddot{\xi}_n(t) + \eta_n S_n \dot{\xi}_n(t) = \frac{1}{\rho_0 h} [p_n(\bar{S}_r^n, t) - p_r(\bar{S}_r^n, t)] ; \quad n = 1, 2, \dots, N \quad (24)$$

Such strongly local damping leads to *complex* (e.g. non-real) acoustical modes for the coupled system. Finally, after modal projection of (22-24) we obtain equation (25), which may be solved using the usual transformation to the first-order form $\{w\} = \langle v, \dot{v} \rangle^T$:

$$[A]\{\ddot{V}(t)\} + [D]\{\dot{V}(t)\} + [B]\{V(t)\} = \{E\} c_0^2 \rho_0 \dot{Q}_s(t) \quad (25)$$

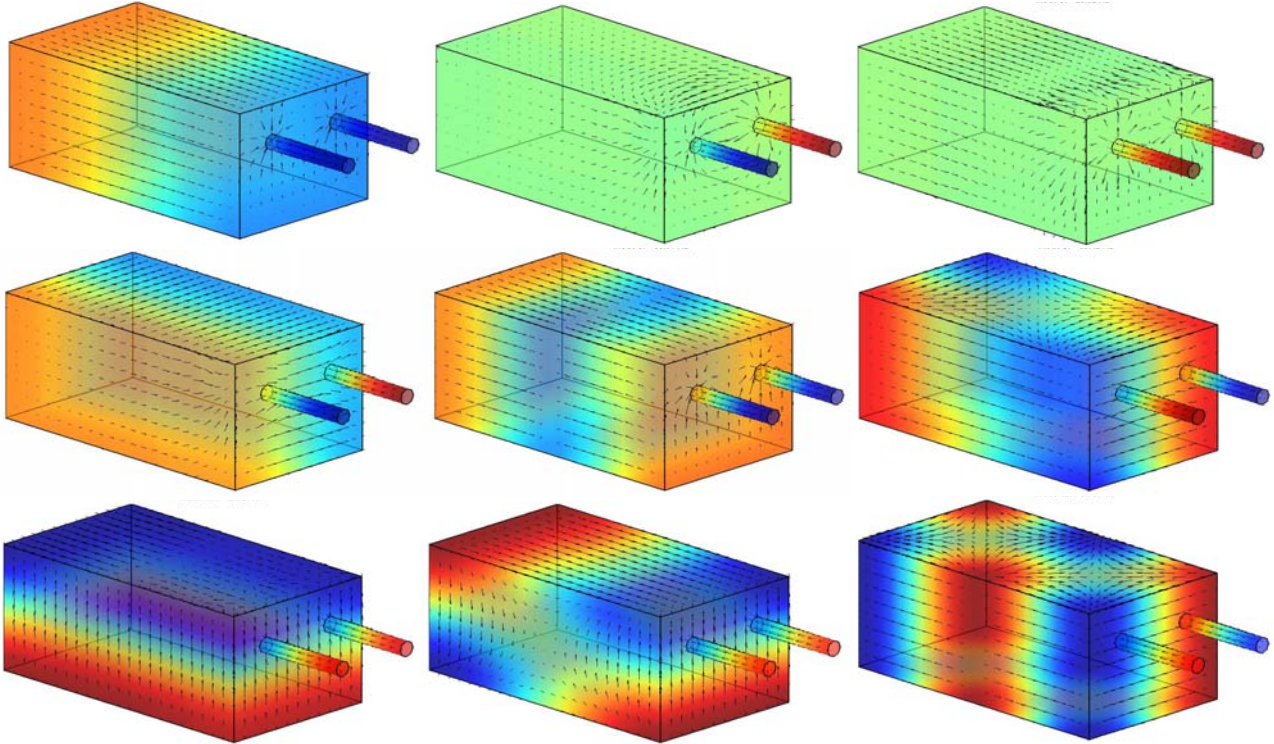


Figure 4.- Modeshapes of the first coupled modes computed using the proposed method

FORCED RESPONSES

To compare the frequency-response functions of the original room with those of the coupled room/resonator(s), the volume-source at excitation location \bar{s}_r^e is assumed harmonic, $Q_s(t) = Q_0 \exp(i\omega t)$, with a sweeping frequency in the range $0 \leq \omega \leq \omega_{\max}$. In steady-state regime, responses will also be harmonic at the excitation frequency, so that the response of the coupled system may be formally written as:

$$\{V(\omega)\} = ([B] + i\omega[D] - \omega^2[A])^{-1} \{E\} i\omega c_0^2 \rho_0 Q_s(\omega) \quad (26)$$

from which the modal and physical responses at any given location \bar{s}_r^e may be computed. For the original uncoupled room, the preceding equations simplify drastically, as they only contain the original room uncoupled modes.

CONCLUSIONS

In this paper we have addressed the problem of computing the modes of a room when coupled to a set of multi-mode resonators, accounting for the viscous dissipative phenomena at the room/resonator interfaces. A simple but representative example was presented and the results compared, for the conservative case, with FEM computations. The modal/sub-structuring technique used here is much less computer-intensive than the finite-element approach. Furthermore, incorporation of dissipative effects is relatively straightforward, the short analysis sketched here being expanded elsewhere. In forthcoming papers we will use the present model for computing the forced responses of coupled room/resonators and optimize the shapes of sets of multi-modal resonators (as well as their locations) to obtain optimal room equalizations.

References

1. K.Ingard: On the Theory and Design of Acoustic Resonators. *Journal of the Acoustical Society of America* **25** (1953) 1037-1061.
2. P.Morse, K.Ingard: Theoretical Acoustics. *Princeton* (1968).
3. R.Chanauud: Effects of Geometry on the Resonance Frequency of Helmholtz Resonators. *Journal of Sound and Vibration* **178** (1994) 337-348.
4. D.Li, J.Vipperman: On the design of long T-shaped acoustic resonators. *Journal of the Acoustical Society of America* **116** (2004) 2785-2792.
5. F.Fahy, C.Schofield: A Note on the Interaction Between a Helmholtz Resonator and an Acoustic Mode of an Enclosure. *Journal of Sound and Vibration* **72** (1980) 365-378.
6. A.Cummings: The Effects of a Resonator Array on the Sound Field in a Cavity. *Journal of Sound and Vibration* **154** (1992) 25-44.
7. O.Inácio, L.Henrique, J.Antunes: Design of Duct Cross-sectional Areas in Bass-Trapping Resonators for Control-Rooms. *Noise Control Engineering Journal* **55** (2007) 172-182.
8. F.Axisa, J.Antunes: Modelling of Mechanical Systems: Fluid-Structure Interaction. *Elsevier* (2007).